

## Article

# Detection of a Peculiar Drift in the Nuclear Radio Jet of the TeV Blazar Markarian 501

Silke Britzen <sup>1,\*</sup>, Gopal Krishna <sup>2</sup>, Emma Kun <sup>3,4,5,6,7</sup>, Héctor Olivares <sup>8</sup>, Ilya Pashchenko <sup>9,10</sup>, Frédéric Jaron <sup>1,11</sup>, Josefa Becerra González <sup>12,13</sup> and David Paneque <sup>14</sup>

- <sup>1</sup> Max-Planck-Institut für Radioastronomie, Auf dem Hügel 69, 53121 Bonn, Germany  
<sup>2</sup> UM-DAE Centre for Excellence in Basic Sciences, Vidyanagari, Mumbai 400098, India  
<sup>3</sup> Theoretical Physics IV: Plasma-Astroparticle Physics, Faculty for Physics & Astronomy, Ruhr University Bochum, 44780 Bochum, Germany  
<sup>4</sup> Ruhr Astroparticle And Plasma Physics Center (RAPP Center), Ruhr-Universität Bochum, 44780 Bochum, Germany  
<sup>5</sup> Astronomical Institute, Faculty for Physics & Astronomy, Ruhr University Bochum, 44780 Bochum, Germany  
<sup>6</sup> Konkoly Observatory, ELKH Research Centre for Astronomy and Earth Sciences, Konkoly Thege Miklós út 15-17, H-1121 Budapest, Hungary  
<sup>7</sup> CSFK, MTA Centre of Excellence, Konkoly Thege Miklós út 15–17, H-1121 Budapest, Hungary  
<sup>8</sup> Department of Astrophysics/IMAPP, Radboud University Nijmegen, P.O. Box 9010, NL-6500 GL Nijmegen, The Netherlands  
<sup>9</sup> Astro Space Center, Lebedev Physical Institute, Russian Academy of Sciences, 119991 Moscow, Russia  
<sup>10</sup> Moscow Institute of Physics and Technology, Dolgoprudny, Institutsky per., 9, 141700 Moscow, Russia  
<sup>11</sup> Department of Geodesy and Geoinformation, TU Wien, Wiedner Hauptstraße 8-10, 1040 Vienna, Austria  
<sup>12</sup> Instituto de Astrofísica de Canarias, Universidad de La Laguna, 38200 La Laguna, Spain  
<sup>13</sup> Departamento de Astrofísica, Universidad de La Laguna, 38206 La Laguna, Spain  
<sup>14</sup> Max Planck Institute for Physics, Föhringer Ring 6, 80805 München, Germany  
\* Correspondence: sbritzen@mpifr.de



**Citation:** Britzen, S.; Krishna, G.; Kun, E.; Olivares, H.; Pashchenko, I.; Jaron, F.; González, J.B.; Paneque, D. Detection of a Peculiar Drift in the Nuclear Radio Jet of the TeV Blazar Markarian 501. *Universe* **2023**, *9*, 115. <https://doi.org/10.3390/universe9030115>

Academic Editor: Ioana Dutan

Received: 5 January 2023

Revised: 14 February 2023

Accepted: 20 February 2023

Published: 23 February 2023



**Copyright:** © 2023 by the authors. Licensee MDPI, Basel, Switzerland. This article is an open access article distributed under the terms and conditions of the Creative Commons Attribution (CC BY) license (<https://creativecommons.org/licenses/by/4.0/>).

**Abstract:** Mrk 501 is one of the most prominent TeV-emitting blazars and belongs to the class of high synchrotron peaked (HSP) blazars. The Doppler factors derived from the jet kinematics are much too low to provide sufficient beaming for the detected high-energy emission (the so-called Lorentz factor crisis). This BL Lac object is also a prime example of a misaligned AGN with an approximately 90° difference in orientation between the inner parsec-scale jet and the kpc-scale jet structure. We have performed a detailed analysis of the pc-scale jet kinematics, based on 23 years of VLBA observations (at 15 GHz) and find, in addition to robustly consolidating the already claimed stationary jet features and a hinted absence of component ejections, a significant drift of the outer nuclear jet. The two outermost jet features move with somewhat higher but still subluminal speeds. Albeit, they move orthogonally to the inner jet, which itself does not partake in the drifting motion. The effect of this intriguing kinematics is that the jet appears strongly curved at first (1995) but then appears to straighten out (2018). To our knowledge, this is the first time that the orthogonal swing of just the outer part of a nuclear jet has been observed. We discuss the possible physical nature of this turning maneuver. In addition, we report evidence for jet emission, which most likely originates in a spine–sheath structure.

**Keywords:** active galactic nuclei; relativistic jets; multiwavelength observations; theoretical emission models; polarization; jet formation; magnetic fields

## 1. Introduction

Markarian 501 (Mrk 501,  $z = 0.034$ ) is a BL Lac Object and belongs to the subgroup of high synchrotron peaked (HSP) blazars. However, when it flares, the low-energy and high-energy peaks move to higher energies, and Mrk 501 can become an extreme high-frequency peaked BL Lac object (EHBL), i.e., a blazar that emits a substantial fraction of its power between the GeV and the TeV bands [1]. Their synchrotron spectrum peaks in the EUV,

X-ray, or MeV band (Ghisellini [2]). This BL Lac object has repeatedly been observed at high flux levels of TeV  $\gamma$ -rays (e.g., [3–6]), and VHE  $\gamma$ -ray spectra in different activity states have been measured [7]. It remains unclear how this high-energy emission is produced and what differentiates such blazars from more typical, i.e., non-HSP or non-EHBL, blazars.

Mrk 501 has been extensively observed in different wavelength regimes to study the physical nature of its emission (e.g., Abdo et al. [5], MAGIC Collaboration et al. [8], Pandey et al. [9,10], Quinn et al. [11]). This BL Lac object is well known for its misaligned radio structure (e.g., van Breugel and Schilizzi [12], Giroletti et al. [13], Conway and Wrobel [14]). van Breugel and Schilizzi [12] reported a gross misalignment between the large-scale (VLA) and small-scale (EVN) structures of the Mrk 501 jet. While EVN observations at 6 cm from 1982 [12] revealed a small (23 mas or 14 pc) one-sided jet at PA 104 deg, possibly curving north-west towards its end, VLA observations performed at 1.3 and 2 cm (1983) show that the nucleus is elongated in PA 54 deg. In 1.6 GHz VSOP observations in 1998 April [15], the jet shows at  $\sim 30$  mas from the core a strong bending accompanied by an abrupt increase in its opening angle (see Figure 8 in [15]), and this widening portion of the pc-scale jet is pointed towards the kpc-scale emission. According to Giroletti et al. [13], Mrk 501 shows several PA changes out to the kpc-scale radio emission.

Many radio interferometric observations have been targeted at this source to study its pc-scale morphology and its evolution (e.g., Giroletti et al. [13], Richards et al. [16], Piner et al. [17], Pushkarev et al. [18], Koyama et al. [19]). The core-dominated radio source reveals a very complex one-sided jet on pc-scales (e.g., Giroletti et al. [13]). Evidence for a spine–sheath structure has also been reported and analyzed based on polarization imaging (e.g., Pushkarev et al. [18], Giroletti et al. [13], and Croke et al. [20]).

Here we present a detailed analysis of the long-term kinematics of the pc-scale jet in order to probe in which respect Mrk 501, and its jet differ from those of standard blazars. The basic parameters of Mrk 501, are listed in Table 1.

**Table 1.** Source name, redshift, SED classification, black hole mass, and distance scale for Mrk 501. Other than the black hole mass, the information was obtained from the MOJAVE webpage.

Object	$z$	Id.	Mass $M_{\odot}$	Scale pc/mas
Mrk 501, 1652 + 398, J1653 + 3945	0.0337	HSP BL Lac	$(0.9\text{--}3.4) \times 10^9$ [21]	0.66

## 2. Observations and Data Reduction

### 2.1. VLBA Data Analysis

We remodeled and reanalyzed a sequence of 36 VLBA observations (15 GHz, MOJAVE<sup>1</sup>) of Mrk 501 taken between the epochs of 1995/01/20 and 2018/06/01. Gaussian circular components were fitted to all the self-calibrated visibility data to obtain the optimum set of component parameters within the *difmap*-modelfit algorithm [22]. The visibilities for each epoch were fitted independently from all the other epochs. The model-fitting procedure was performed blindly so as not to impose any specific structural outcome. Special care was taken to correctly identify the brightest component as the core component in every individual data set.

### 2.2. Uncertainty Estimation

To obtain conservative uncertainty estimates of the model component parameters, we employed the results of Kravchenko et al. (in prep.). They adopted the basic approach of [23] and calibrated it using several sources from the MOJAVE sample displaying a tight power-law dependence of the component brightness temperature  $T_b$  vs. component size  $R$ , accounting for the residual uncertainty in the amplitude scale at each epoch. The obtained uncertainties are conservative (i.e., upper limits) because some dispersion in the observed  $T_b(R)$  dependence could be of intrinsic origin. This is similar to the method of Lister et al. [24] for estimating the positional uncertainty of the model components from the fit to the multi-epoch kinematical data.

An additional positional error of the components across the epochs could possibly arise due to the core shuttle effect [25,26]. This uncertainty is expected to be quite small ( $\sim 0.1$  mas) and would shift components only in the direction *along* the jet. Any error in the core alignment at different epochs would again only increase the uncertainties *along* the jet direction. Mrk 501 reveals a very complex jet structure as seen in VSOP observations at 1.6 GHz [15]. The structure seen in 15 GHz VLBA observations appears more compact. Future deeper images might reveal the sub-structure of the outer jet investigated here.

### 2.3. Component Identification

We identified the jet components according to their position in the jet and their specific and discriminating kinematic properties. The main jet ridge line is the dominant structure and comprised of a chain of jet components. Components that belong to this main jet ridge line remain at similar core separations with time. These are components j3–j6. j1 and j2 denote the outermost components appearing at a larger distance from the core as well as from the main jet ridge line. j1 and j2 reveal motion towards the main jet ridge line. j3–j6 are the components that define the main jet ridge line, and r\_sheath and l\_sheath are features straddling the main jet ridge line on the two sides, with some gap in between. The r\_sheath and l\_sheath components appear at a rather constant separation on both sides of the main ridge line.

### 3. Results

We confirm the structural complexity of the jet on pc-scales (e.g., Giroletti et al. [13]) and additionally find that the pc-scale structure has varied markedly between 1995 and 2018, as can be seen in Figure 1a,b. Further maps are shown in Figures A1–A4 in the Appendix A. In all of these maps, the model-fit Gaussian components are labeled. Figure 1a,b depicts the pc-scale morphology (with the Gaussian model-fit components superimposed) obtained from the two epochs' data. While the jet appears curved in 1995 (Figure 1a), it largely straightened out by 2018 (Figure 1b). This is also seen in Figure 2a, where we display the positions of the jet features at different epochs (in x-y coordinates). In Figure 2b, we display those jet features whose positions were traceable across the epochs.

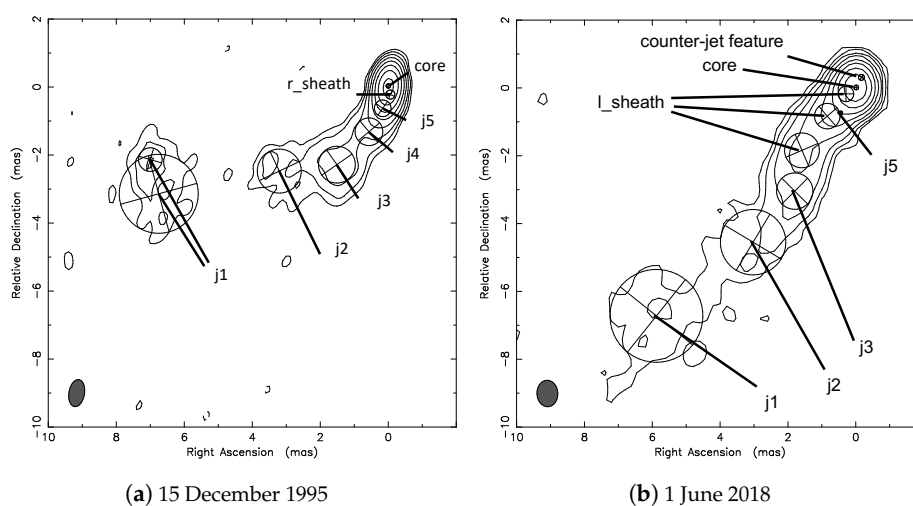
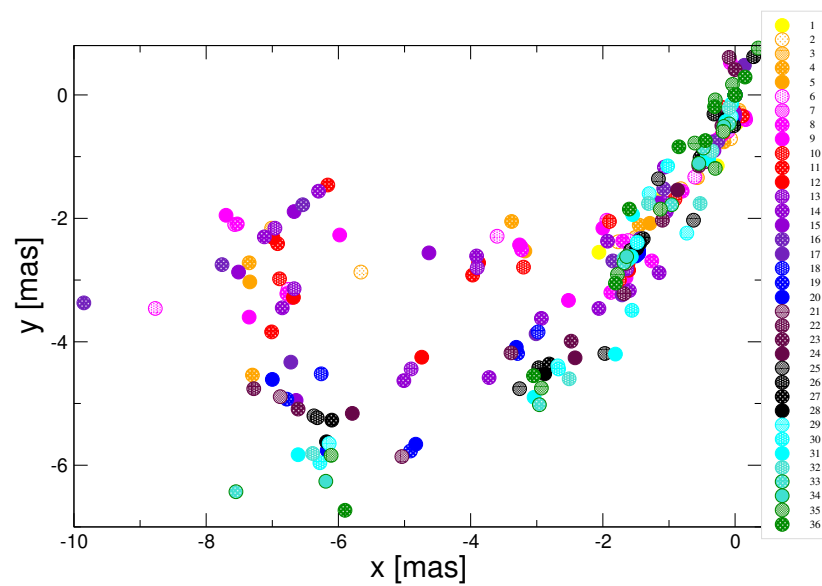
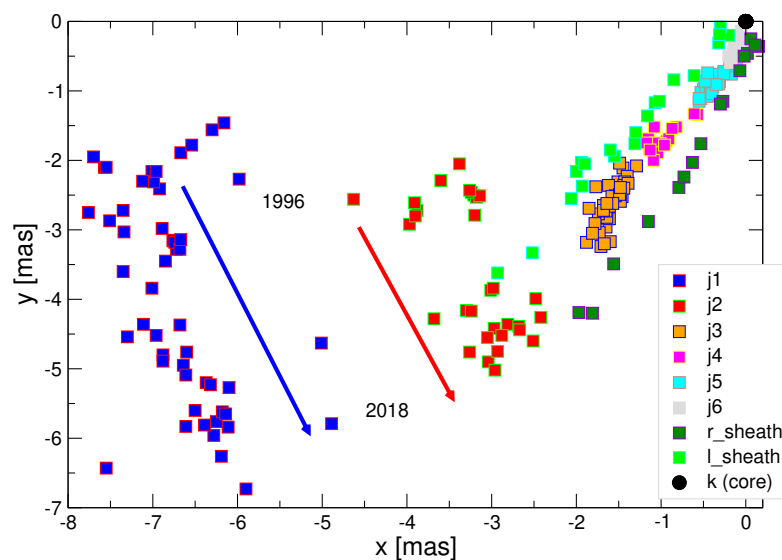


**Figure 1.** The jet mapped with the VLBA at 15 GHz at two different epochs. (a) The pc-scale structure observed on 15 December 1995 and (b) as observed on 1 June 2018. In both maps, we have labeled the model-fit Gaussian components. Note that not every jet component is identifiable in each observation. While the jet appears strongly curved in (a), it appears essentially straight in (b).



(a)



(b)

**Figure 2.** (a) The evolution of the x-y coordinates of the jet features modeled for all of the 36 epochs. The different epochs are indicated with different colors (1: the first/earliest epoch, 36: the latest/youngest epoch). (b) Same figure as in (a), but showing only those features that could be identified and tracked across the epochs. In addition to the jet features (j3–j6), which most likely define the spine, we indicate in light-green and purple those jet components that might belong to the sheath (l\_sheath, r\_sheath). The two outermost jet features (j1 and j2) are clearly seen to move, and their motion is indicated by arrows along which the range and progression of the epochs covered are also shown.

While the inner two mas of the jet appear rather well collimated, the outer part of the nuclear jet (beyond  $\sim 2$  mas) appears much less confined. The two outermost jet features

appear to move from smaller (negative) y-values to larger (negative) y-values. This motion is indicated in Figure 2b by the two arrows.

We confirm the stationarity of jet features (j3–j6) with regard to the core distance, as reported by other authors before, e.g., [15,27]. The proper motions and apparent speeds, as well as the general directions of motion for all those components that could be traced are listed in Table 2. The proper motions have been determined via linear regression performed for the radial distance to the core data, as shown in Figure 3. However, for the components j1 and j2, we followed a different approach to determine the proper motion. Here, we fitted the proper motion for  $x(t)$  and  $y(t)$  independently according to  $x(t) = x_0 + \mu_x \times t$  and  $y(t) = y_0 + \mu_y \times t$ . We then determined the total proper motion by taking their quadratic sum  $\mu_{tot} = \sqrt{\mu_x^2 + \mu_y^2}$ , Homan et al. [28].

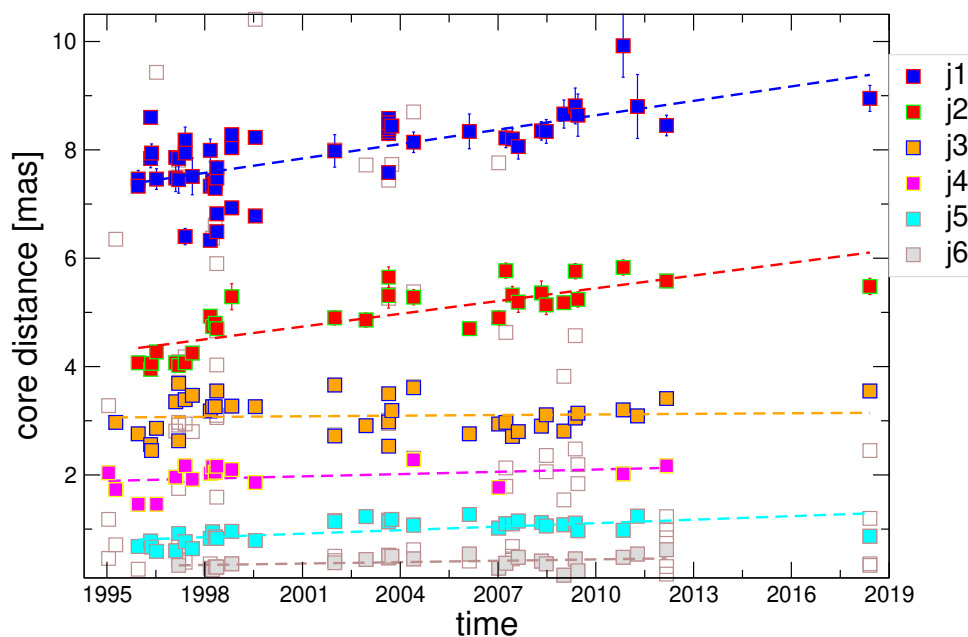


**Figure 3.** Temporal evolution of the separation from the core is shown for the moving jet components (j1, j2) and for the stationary jet features (j3–j6). The color scheme is the same as in Figure 2b. Unfilled squares (brown) denote jet features from the sheath structure and those jet features that could not be identified reliably. Dashed lines indicate a linear regression fit to the data points shown here.

**Table 2.** Component identification, proper motion in the x-coordinate, proper motion in the y-coordinate, total proper motion, apparent speeds, and the direction of motion.

Jet Component	$\mu_x$ (mas/yr)	$\mu_y$ (mas/yr)	Total p.m. (mas/yr)	App.Speed [c]	Direction of Motion
j6			$0.009 \pm 0.005$	$0.02 \pm 0.01$	along the jet
j5			$0.022 \pm 0.005$	$0.05 \pm 0.01$	" "
j4			$0.014 \pm 0.011$	$0.03 \pm 0.02$	" "
j3			$0.004 \pm 0.010$	$0.01 \pm 0.02$	" "
j2	$0.048 \pm 0.013$	$-0.151 \pm 0.012$	$0.158 \pm 0.018$	$0.35 \pm 0.04$	orthogonal to the jet
j1	$0.045 \pm 0.014$	$-0.239 \pm 0.022$	$0.243 \pm 0.026$	$0.54 \pm 0.06$	" "

### 3.1. Spine–Sheath Structure

Figure 2b shows that the jet features j3–j6 are well-aligned along the main jet ridge line. These jet features most likely define the spine of the jet. On both sides of this spine, jet features straddling this spine can be seen (r\_sheath, l\_sheath). These features probably represent the sheath around the jet. A spine–sheath jet structure in this pc-scale jet has been

reported earlier, based on polarization maps (e.g., Pushkarev et al. [18], Giroletti et al. [13], and Croke et al. [20]).

### 3.2. Close to the 15 GHz Core

We confirm the previously reported ‘off-axis’ jet structure close to the core [19]. Additionally, on the counter-jet side, we find evidence for jet features that most likely are counter-jet components extending up to 0.8 mas in the y-coordinate (Figure 2a). Details of both these features—the off-axis jet structure, as well as the counter-jet components—are subject to another study (Britzen et al., in prep.).

## 4. Discussion

Mrk 501 is considered to be a prototypical TeV blazar, but it has shown two characteristics that differentiates it from the other gamma-ray blazars. On the one hand, despite being classified as an HBL, Mrk 501 behaved as an extreme high-frequency-peaked blazar (EHBL) throughout the entire 2012 observing season [1]: the synchrotron peak was measured to lie above 5 keV and the inverse-Compton peak above 0.5 TeV during all the observations (e.g., during both high and low activity). On the other hand, Mrk 501 is the only blazar known so far, which has shown a hint of multiple spectral components in the VHE gamma-ray energy range. During July 2014, the MAGIC telescopes detected evidence of an additional narrow spectral component superposed on the broadband emission [8]. This narrow spectral component has a significance of 3–4  $\sigma$  with respect to a single emission component, and it is centered around 3 TeV. The detection of this component occurred in coincidence with the strongest Mrk 501 flare in the X-ray band detected during the 17-year-long operation of the Neil Gehrels Swift observatory. The detection of this transient spectral feature makes Mrk 501 a particularly interesting target to search for jet structures, especially in radio, where the current instrumentation has the resolution to detect and follow the temporal evolution of multiple components.

### 4.1. Apparent Stationarity of Jet Features and a Long Spell of No Component Ejection

Several kinematical studies of the pc-jet of Mrk 501 have revealed apparent stationarity of the jet components. Giroletti et al. [15] found no proper motion in any of the four components observed by them at 15 GHz. Edwards and Piner [27] report two subluminal and two stationary components based on VLBA data obtained at 8 and 15 GHz between 1995 and 1999. The MOJAVE team [29,30] listed values for the proper motion of eight jet components with values ranging from  $12.8 \pm 6.8 \mu\text{as}/\text{y}$  ( $0.029 \pm 0.015 c$ ) to  $397 \pm 78 \mu\text{as}/\text{y}$  ( $0.89 \pm 0.17 c$ ). We find that the jet features j3–j6 move with subluminal speeds (see Table 2) and confirm the slow apparent speeds reported before.

A striking new feature emerging from the present study is that we find no component ejections during the entire 23 years of VLBA observations analyzed here. This contrasts with more typical (i.e., non-extreme) blazars where apparent superluminal motion is commonly observed, and “new” components seem to be ejected from the core quasi-regularly on year-like time scales. Edwards and Piner [27] highlight the fact that no new component has emerged from the core of Mrk 501, after its high TeV state in 1997 (till July 1999). They suggest that events related to extended TeV (and accompanying X-ray) activity are decoupled from those producing new VLBI components (e.g., [31]). The much longer dataset analyzed here appears to consolidate this hypothesis.

Jet components that maintain the same core separation, not showing the classical outward-directed motion, are expected for helical jets seen under a small line-of-sight angle (inclination). The best example where a dependence of the jet component’s apparent speed on the viewing angle has been studied is the BL Lac Object PKS 0735+178 [32]. The source is a helical jet and revealed apparent superluminal motion of its jet components for five years. The source then switched into a seven-year phase of apparent stationarity of jet components. During this time, no component ejections were found. Further scrutiny of the literature revealed that the source had shown a similar transiting behavior already in

earlier observations. Britzen et al. [32] explain these findings by a (most likely curling) jet with a changing viewing angle.

For Mrk 501, further observations, preferably at higher frequencies, are required to clarify the physical cause of the apparent stationarity of components. Most likely, a helical jet and/or helical magnetic field and special viewing angle play a role.

#### 4.2. A Turning Maneuver of the Jet

Another striking feature of Mrk 501 found here is the observed “drift” of the pc-scale jet at 15 GHz. Remarkably, the drift is limited to the outer part (beyond 2 mas distance from the core). The two outermost jet features move with somewhat higher speeds, albeit *orthogonally to the inner jet, which does not partake in the drift*. In the following, we discuss the possible origin of the jet’s turning maneuver.

Previous observations (e.g., Giroletti et al. [15]) have shown that the inner jet extends at a PA of  $\sim 145$ – $155$  deg, finally bending towards a PA of  $\sim 45$  deg. This latter PA is in agreement with the lower-resolution VLA images. As VSOP observations revealed [15], at this bending region, the jet spreads and forms a cone-shaped diffuse emission. This could be due to an interaction with the surrounding medium. It has been suggested that such interactions might bend the jet trajectory (e.g., [33]). According to another explanation [14], a helical jet could explain the complex jet morphology as well as the misalignment between the pc- and kpc-scale radio structure.

The MOJAVE spectral index image between 8 and 15 GHz displays relatively flatter spectra at the upper portion of the inner jet ( $< 2$  mas from the core) [34]. The jet also displays limb brightening both before and after its large (projected) bend (starting at about 30 mas distance from the core) [15], although other authors do not confirm the limb brightening for parts of the jet [20]. According to Gabuzda [35], limb brightening in Mrk 501 is most likely related to some intrinsic property of the jet propagating through an ambient medium, such as a helical B field, mass loading or particle acceleration at the jet’s edges. However, limb brightening can also be caused by differential Doppler boosting [15,36]. Alternate theories explain limb brightening by efficient particle acceleration at sheared boundary layers [37,38].

Polarization data might help to unravel the origin of the complex radio structure and unusual kinematics of this jet. In this manuscript, we report evidence for a spine–sheath structure based on total intensity imaging. A comparison between the spine–sheath structure properties derived in this paper and the spine–sheath structure derived by [18] based on polarization data is beyond the scope of this paper but planned for a future publication. Since the polarization is variable, a detailed analysis will be required. Based on a visual inspection of the polarization maps of Mrk 501, provided by the MOJAVE team, it seems that parts of the jet indicate a spine–sheath polarization structure. The fractional polarization increases towards the jet edges. The latter can either be explained by a helical jet B field or shocks along the jet ridge line combined with shear at the jet edges (e.g., [35]). The CLEAN bias could also contribute to the increase in the fractional polarization towards the edges [39]. Croke et al. [20] obtained the first rotation measure (RM) map based on a joint analysis of polarization data at 1.6, 2.2, 5, and 8 GHz. They find a clear systematic gradient in the RM across the VLBI jet. This transverse gradient extends from the core region to a distance of  $\sim 30$  mas from the core. The authors interpret this finding as support for the hypothesis that a helical magnetic field is associated with the jet of Mrk 501. The RM gradient could also be produced in the outer sheath wrapping around the jet, as observations of 3C 273 have revealed [40].

We find motion in the outer, diffuse (conical) part of the jet. The direction of this motion coincides with the expected direction of motion in case the motion is caused by a helical magnetic field. Thus, while there are several arguments that point in favor of an explanation in terms of a helical magnetic field governing the drift of the outer components, there are other arguments that deserve consideration, as well.

The motion in the outer part of the jet is not directed towards the large-scale PA of  $\sim 45^\circ$  but in the opposite direction. While this large-scale PA could also result from an earlier orientation of the Mrk 501 central engine, which might have changed due to a merger and consequent spin-flip (e.g., [41]), this finding argues against a helical magnetic field as the origin of this diffuse feature. Another argument against the helical magnetic field comes from the fact that only the outer portion of the nuclear jet is drifting while the inner jet remains steady. Interaction of the jet with the surrounding medium thus seems to be a more plausible explanation, as compared to the possibility of a drifting axis of the central engine. This distinction would be much harder to make in the case of most blazars, which lie at greater distances, and hence their nuclear jets are not so well resolved.

In reality, the process behind the jet's drift is likely to be more complex than a bend due to a collision with a denser region in the ambient medium. The visual comparison with the MOJAVE polarization data indicates the existence of two locations with a pronounced change in polarization, suggesting a helical structure, as noted above, can originate through several mechanisms. Such helical pattern may appear as a result of the current-driven kink instability, which has been proposed as a strong candidate for accelerating particles via turbulent magnetic reconnection, producing the very high energy emission (GeV-TeV) observed in blazars [42,43]. Such an origin of the helical pattern would be consistent with the jet propagating in a straight direction until the turning maneuver, where the instability enters a nonlinear regime. Identification of the source of TeV flares with such turning points in their pc-scale jets would favor this hypothesis.

Another possibility that deserves attention is precession at the jet base that goes unnoticed near to the core due to an observing angle that is small compared to the opening angle of the helix [14]. Precessing jets have been shown to arise in general relativistic magnetohydrodynamic simulations due to the Lense–Thirring effect when the spin of the black hole is misaligned with the larger scale angular momentum of the accretion flow (see, e.g., [44]). Simulations of accretion onto binary black holes with mass ratios from 1:1 to 1:10 separated by 10 gravitational radii,  $r_g = GM/c^2$ , have shown that the jets from the two black holes merge into a single helical structure at relatively small distances (of the order of  $100 r_g$ ) [45]. Both of these scenarios would be favored if additional phenomenology were discerned, such as a measurable drift in the inner part of the jet, periodicities in the light curve, or emission associated with spiral shocks in the innermost accretion flow.

We observe stationary jet features for the inner part of the jet and larger apparent speeds in the outer part of the jet. An intrinsic bend could help to explain the observations. According to the work by Giroletti et al. [13], it is possible that the jet is more closely aligned in its inner part and is oriented at a larger viewing angle after the turn. The drift may also come from some twist produced at the jet base that propagates away, changing the direction at larger radii. There is some evidence for a mildly wavy pattern over the entire first 7 mas length, starting from the core (Figure 1b). The drift could also be caused by changes in the ambient medium. Determining the exact cause of the drift may require more detailed modeling and additional input from polarimetric data.

To summarize, this study reports some unusual new properties of the pc-scale radio jet of Mrk 501. While a direct causal connection between the drifting motion of the outer VLBI jet, the stationary inner knots, the prolonged absence of component ejections and concrete observed TeV-flares could not be robustly detected (no 15 GHz data available near the epoch of, e.g., the 2014 flare), a comprehensive understanding of the wide-ranging observational peculiarities of Mrk 501 would be feasible by taking into account the entire gamut of multi-band temporal, polarimetric and kinematical complexities of this remarkable blazar. The present study adds further new pieces to the puzzle of this enigmatic object. Further investigations of these observational findings are planned and will be reported in a forthcoming paper.

**Author Contributions:** S.B. performed the data analysis, prepared the images, and drafted the paper; G.K. improved this manuscript by providing insightful comments and editing the manuscript; E.K., H.O., and F.J. helped with the interpretation of the observations and editing of the manuscript; I.P. performed the uncertainty analysis and cosmology checks; J.B.G. and D.P. contributed with their expertise concerning the theoretical interpretation of the results. All authors have read and agreed to the published version of the manuscript.

**Funding:** I.P. was supported by the Russian Science Foundation (project 20-72-10078).

**Data Availability Statement:** The data presented in this study are available on request from the corresponding author.

**Acknowledgments:** We thank Nicholas Roy MacDonald for valuable discussions and many helpful comments that improved the paper. We are grateful to the three anonymous referees for their thoughtful questions and suggestions. This research has made use of data from the MOJAVE database, which is maintained by the MOJAVE team [46]. G.K. thanks the Indian National Science Academy for a Senior Scientist fellowship. E. Kun acknowledges support from the German Science Foundation DFG, via the Collaborative Research Center *SFB1491: Cosmic Interacting Matters—From Source to Signal*. E.K. thanks the Hungarian Academy of Sciences for its Premium Postdoctoral Scholarship. This research was funded in part by the Austrian Science Fund (FWF) (P31625).

**Conflicts of Interest:** The authors declare no conflict of interest.

## Abbreviations

The following abbreviations are used in this manuscript:

AGN	active galactic nucleus
SED	spectral energy distribution
VLBI	very long baseline interferometry
VLBA	very long baseline array
VLA	very large array
VHE	very high energy
HBL	high-frequency peaked BL Lac object
HSP	high synchrotron peaked blazar
EHBL	extreme high-frequency peaked BL Lac object
HSP	high-synchrotron-peaked BL Lac
MAGIC	major atmospheric gamma-ray imaging Cherenkov telescopes
EVN	European VLBI network
MOJAVE	monitoring of jets in active galactic nuclei with VLBA experiments
SMBBH	supermassive binary black hole
SSC	self synchrotron compton
Mrk	Markarian
VSOP	VLBI Space observatory program
RM	rotation measure
PA	position angle
BH	black hole

Appendix A. All Maps of Mrk 501

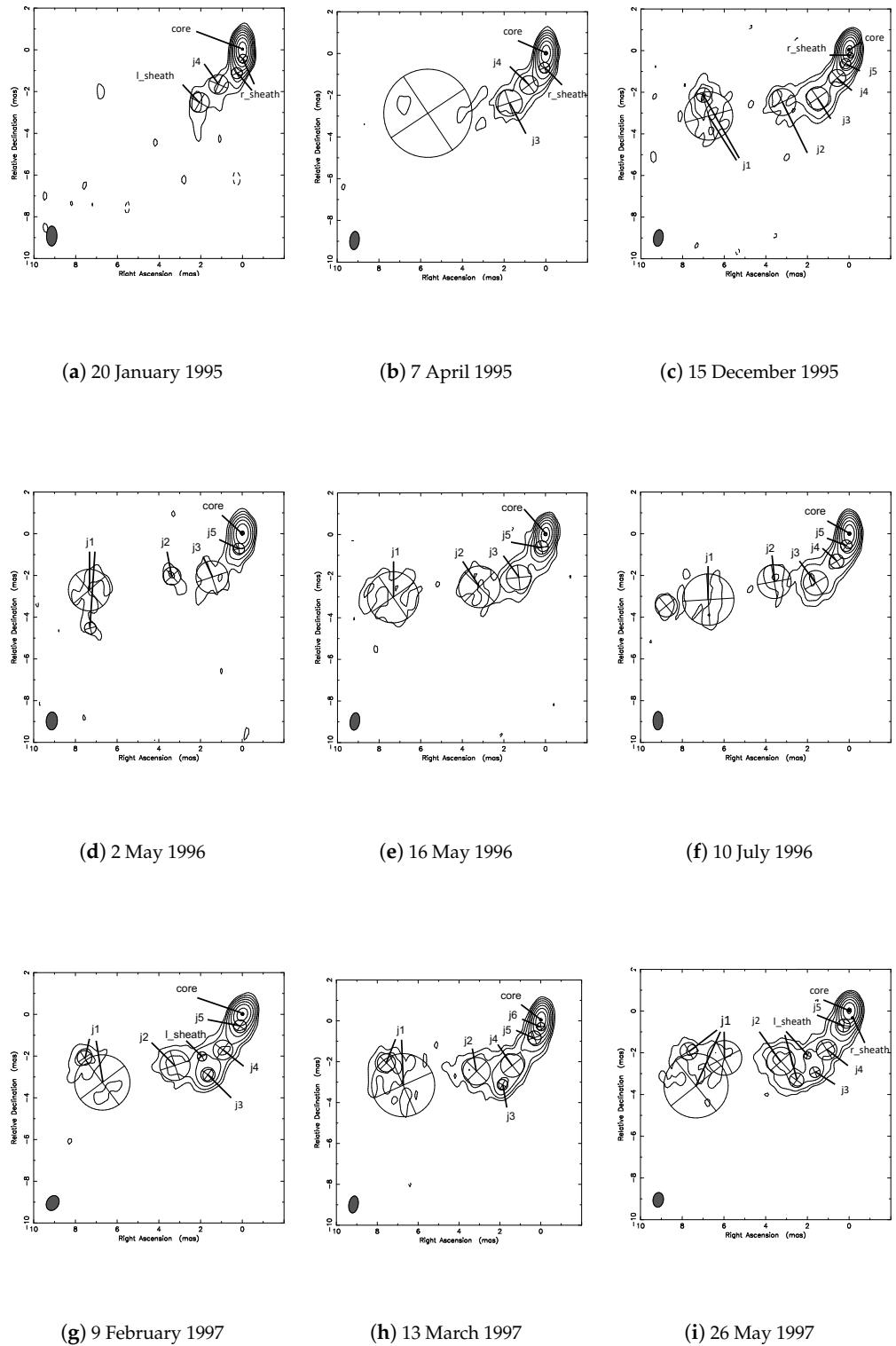
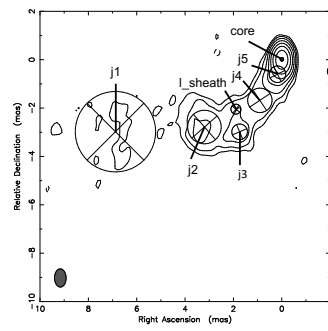
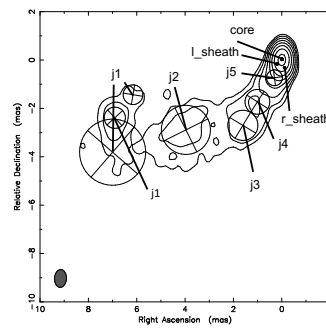


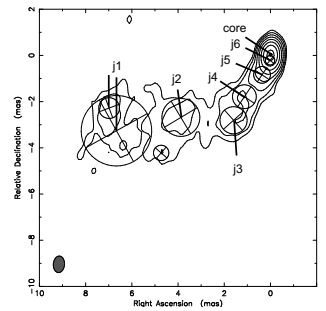
**Figure A1.** The jet mapped with the VLBA at 15 GHz at nine different epochs between 20 January 1995 and 26 May 1997. Superimposed are the labels of the model-fit Gaussian components. Note that not every jet component is identifiable in each observation.



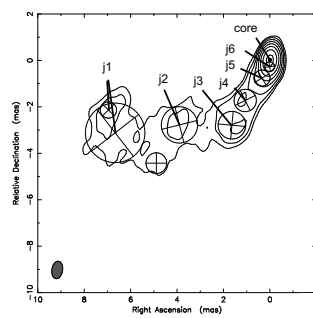
(a) 15 August 1997



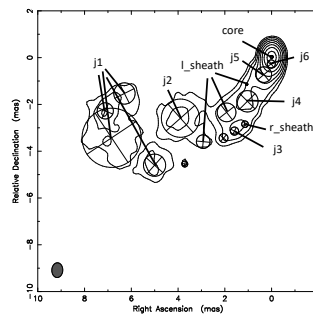
(b) 4 March 1998



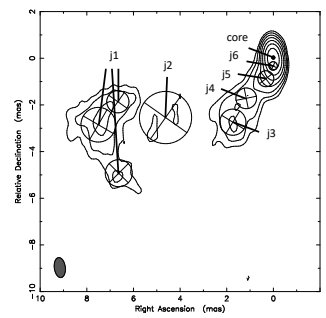
(c) 28 March 1998



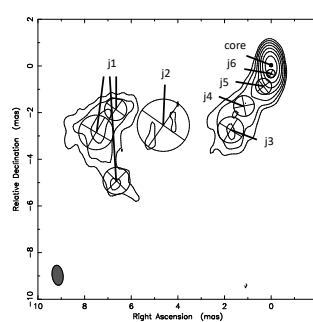
(d) 26 April 1998



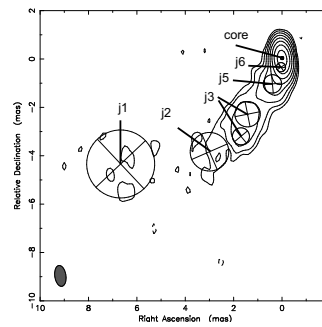
(e) 15 May 1998



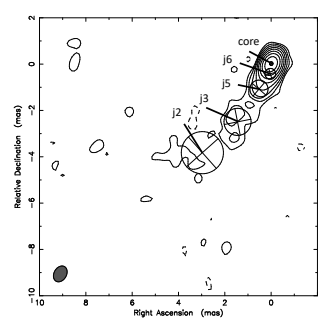
(f) 30 October 1998



(g) 19 July 1999



(h) 30 December 2001



(i) 13 December 2002

Figure A2. Same as in Figure A1 for the nine epochs between 15 August 1997 and 13 December 2002.

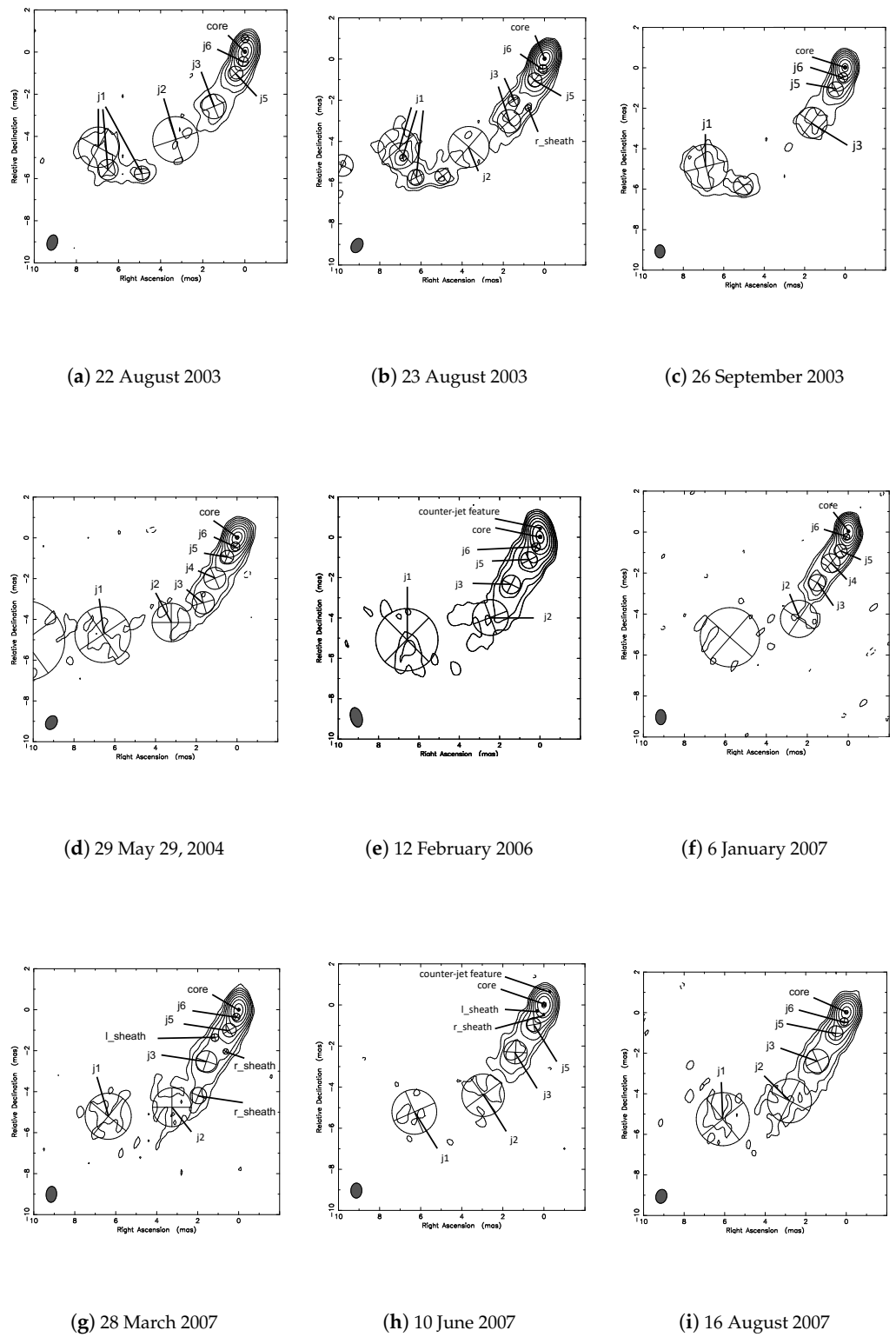
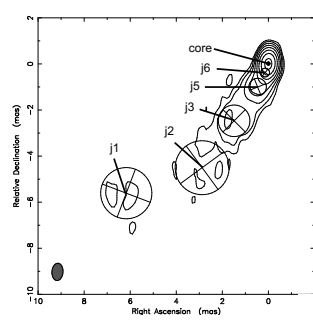
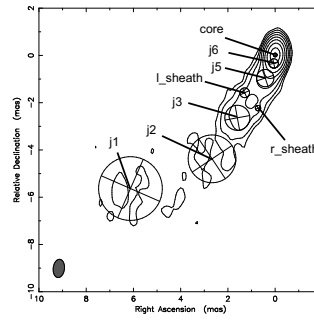


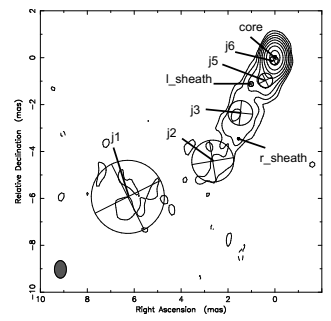
**Figure A3.** Same as in Figures A1 and A2 for the nine epochs between 22 August 2003 and 16 August 2007.



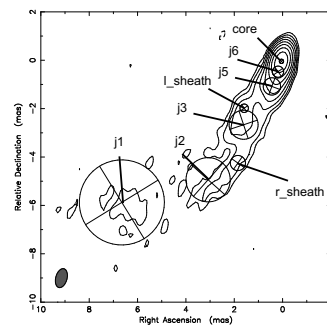
(a) 1 May 2008



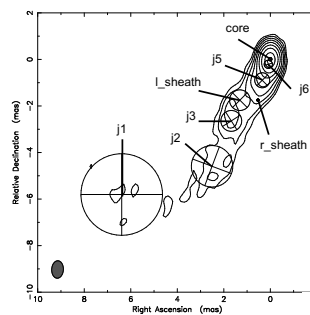
(b) 25 June 2008



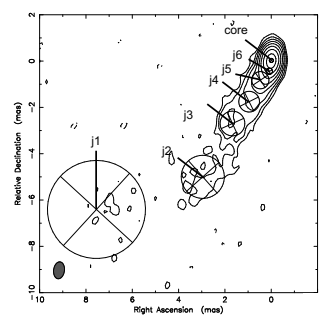
(c) 7 January 2009



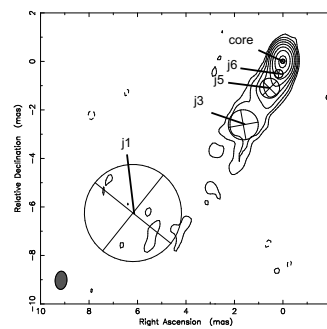
(d) 14 May 2009



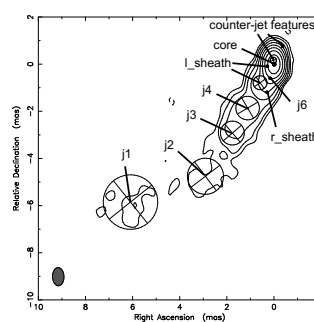
(e) 15 June 2009



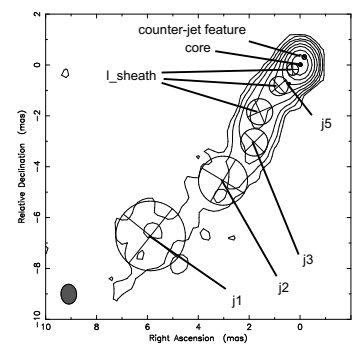
(f) 4 November 2010



(g) 11 April 2011



(h) 4 March 2012



(i) 1 June 2018

Figure A4. Same as in Figures A1–A3 for the nine epochs between 1 May 2008 and 1 June 2018.

## Notes

- <sup>1</sup> Monitoring Of Jets in Active galactic nuclei with VLBA Experiments webpage, see <https://www.cv.nrao.edu/MOJAVE/>, accessed on 14 December 2021.

## References

- Ahnen, M.L.; Ansoldi, S.; Antonelli, L.A.; Arcaro, C.; Babić, A.; Banerjee, B.; Bangale, P.; Barres de Almeida, U.; Barrio, J.A.; Becerra González, J.; et al. Extreme HBL behavior of Markarian 501 during 2012. *Astron. Astrophys.* **2018**, *620*, A181. [[CrossRef](#)]
- Ghisellini, G. Extreme blazars. *Astropart. Phys.* **1999**, *11*, 11–18. [[CrossRef](#)]
- Aharonian, F.; Akhperjanian, A.G.; Barrio, J.A.; Bernlöhr, K.; Bojahr, H.; Calle, I.; Contreras, J.L.; Cortina, J.; Daum, A.; Deckers, T.; et al. The temporal characteristics of the TeV gamma -emission from MKN 501 in 1997. II. Results from HEGRA CT1 and CT2. *Astron. Astrophys.* **1999**, *349*, 29–44.
- Aharonian, F.A.; Akhperjanian, A.G.; Barrio, J.A.; Bernlöhr, K.; Bojahr, H.; Calle, I.; Contreras, J.L.; Cortina, J.; Daum, A.; Deckers, T.; et al. The time averaged TeV energy spectrum of MKN 501 of the extraordinary 1997 outburst as measured with the stereoscopic Cherenkov telescope system of HEGRA. *Astron. Astrophys.* **1999**, *349*, 11–28.
- Abdo, A.A.; Ackermann, M.; Ajello, M.; Allafort, A.; Baldini, L.; Ballet, J.; Barbiellini, G.; Baring, M.G.; Bastieri, D.; Bechtol, K.; et al. Insights into the High-energy  $\gamma$ -ray Emission of Markarian 501 from Extensive Multifrequency Observations in the Fermi Era. *Astrophys. J.* **2011**, *727*, 129. [[CrossRef](#)]
- Arbet-Engels, A.; Baack, D.; Balbo, M.; Biland, A.; Bretz, T.; Buss, J.; Dorner, D.; Eisenberger, L.; Elsaesser, D.; Hildebrand, D.; et al. Long-term multi-band photometric monitoring of Mrk 501. *Astron. Astrophys.* **2021**, *655*, A93. [[CrossRef](#)]
- Anderhub, H.; Antonelli, L.A.; Antoranz, P.; Backes, M.; Baixeras, C.; Balestra, S.; Barrio, J.A.; Bastieri, D.; Becerra González, J.; Becker, J.K.; et al. Simultaneous Multiwavelength Observation of Mkn 501 in a Low State in 2006. *Astrophys. J.* **2009**, *705*, 1624–1631. [[CrossRef](#)]
- MAGIC Collaboration; Acciari, V.A.; Ansoldi, S.; Antonelli, L.A.; Babić, A.; Banerjee, B.; Barres de Almeida, U.; Barrio, J.A.; Becerra González, J.; Bednarek, W.; et al. Study of the variable broadband emission of Markarian 501 during the most extreme Swift X-ray activity. *Astron. Astrophys.* **2020**, *637*, A86. [[CrossRef](#)]
- Pandey, A.; Gupta, A.C.; Wiita, P.J. X-ray Intraday Variability of Five TeV Blazars with NuSTAR. *Astrophys. J.* **2017**, *841*, 123. [[CrossRef](#)]
- Pandey, A.; Gupta, A.C.; Wiita, P.J. X-ray Flux and Spectral Variability of Six TeV Blazars with NuSTAR. *Astrophys. J.* **2018**, *859*, 49. [[CrossRef](#)]
- Quinn, J.; Akerlof, C.W.; Biller, S.; Buckley, J.; Carter-Lewis, D.A.; Cawley, M.F.; Catanese, M.; Connaughton, V.; Fegan, D.J.; Finley, J.P.; et al. Detection of Gamma Rays with  $E > 300$  GeV from Markarian 501. *Astrophys. J. Lett.* **1996**, *456*, L83. [[CrossRef](#)]
- van Breugel, W.; Schilizzi, R. VLBI and VLA Observations of the BL Lacertae-Type Object Markarian 501: Evidence for Grossly Misaligned Small-Scale and Large-Scale Radio Structure. *Astrophys. J.* **1986**, *301*, 834. [[CrossRef](#)]
- Giroletti, M.; Giovannini, G.; Cotton, W.D.; Taylor, G.B.; Pérez-Torres, M.A.; Chiaberge, M.; Edwards, P.G. The jet of Markarian 501 from millions of Schwarzschild radii down to a few hundreds. *Astron. Astrophys.* **2008**, *488*, 905–914. [[CrossRef](#)]
- Conway, J.E.; Wrobel, J.M. A Helical Jet in the Orthogonally Misaligned BL Lacertae Object Markarian 501 (B1652+398). *Astrophys. J.* **1995**, *439*, 98. [[CrossRef](#)]
- Giroletti, M.; Giovannini, G.; Feretti, L.; Cotton, W.D.; Edwards, P.G.; Lara, L.; Marscher, A.P.; Mattox, J.R.; Piner, B.G.; Venturi, T. Parsec-Scale Properties of Markarian 501. *Astrophys. J.* **2004**, *600*, 127–140. [[CrossRef](#)]
- Richards, J.L.; Max-Moerbeck, W.; Pavlidou, V.; King, O.G.; Pearson, T.J.; Readhead, A.C.S.; Reeves, R.; Shepherd, M.C.; Stevenson, M.A.; Weintraub, L.C.; et al. Blazars in the Fermi Era: The OVRO 40 m Telescope Monitoring Program. *Astrophys. J. Suppl.* **2011**, *194*, 29. [[CrossRef](#)]
- Piner, B.G.; Pant, N.; Edwards, P.G. The Jets of TeV Blazars at Higher Resolution: 43 GHz and Polarimetric VLBA Observations from 2005 to 2009. *Astrophys. J.* **2010**, *723*, 1150–1167. [[CrossRef](#)]
- Pushkarev, A.B.; Gabuzda, D.C.; Vetukhnovskaya, Y.N.; Yakimov, V.E. Spine-sheath polarization structures in four active galactic nuclei jets. *Mon. Not. RAS* **2005**, *356*, 859–871. [[CrossRef](#)]
- Koyama, S.; Kino, M.; Giroletti, M.; Doi, A.; Giovannini, G.; Orienti, M.; Hada, K.; Ros, E.; Niinuma, K.; Nagai, H.; et al. Discovery of off-axis jet structure of TeV blazar Mrk 501 with mm-VLBI. *Astron. Astrophys.* **2016**, *586*, A113. [[CrossRef](#)]
- Croke, S.; O’Sullivan, S.; Gabuzda, D. The parsec-scale distributions of intensity, linear polarization and Faraday rotation in the core and jet of Mrk501 at 8.4–1.6 GHz. *Mon. Not. R. Astron. Soc.* **2009**, *402*, 259–270. [[CrossRef](#)]
- Barth, A.J.; Ho, L.C.; Sargent, W.L.W. Stellar Velocity Dispersion and Black Hole Mass in the Blazar Markarian 501. *Astrophys. J. Lett.* **2002**, *566*, L13–L16. [[CrossRef](#)]
- Shepherd, M.C. Difmap: An Interactive Program for Synthesis Imaging. In *Proceedings of the Astronomical Data Analysis Software and Systems VI*; Astronomical Society of the Pacific Conference Series; Hunt, G., Payne, H., Eds.; Astronomical Society of the Pacific: San Francisco, CA, USA, 1997; Volume 125, p. 77.
- Lee, S.S.; Lobanov, A.P.; Krichbaum, T.P.; Witzel, A.; Zensus, A.; Bremer, M.; Greve, A.; Grewing, M. A Global 86 GHz VLBI Survey of Compact Radio Sources. *Astron. J.* **2008**, *136*, 159–180. [[CrossRef](#)]

24. Lister, M.L.; Cohen, M.H.; Homan, D.C.; Kadler, M.; Kellermann, K.I.; Kovalev, Y.Y.; Ros, E.; Savolainen, T.; Zensus, J.A. MOJAVE: Monitoring of Jets in Active Galactic Nuclei with VLBA Experiments. VI. Kinematics Analysis of a Complete Sample of Blazar Jets. *Astron. J.* **2009**, *138*, 1874–1892. [[CrossRef](#)]
25. Lisakov, M.M.; Kovalev, Y.Y.; Savolainen, T.; Hovatta, T.; Kutkin, A.M. A connection between  $\gamma$ -ray and parsec-scale radio flares in the blazar 3C 273. *Mon. Not. RAS* **2017**, *468*, 4478–4493. [[CrossRef](#)]
26. Plavin, A.V.; Kovalev, Y.Y.; Pushkarev, A.B.; Lobanov, A.P. Significant core shift variability in parsec-scale jets of active galactic nuclei. *Mon. Not. RAS* **2019**, *485*, 1822–1842. [[CrossRef](#)]
27. Edwards, P.G.; Piner, B.G. The Subluminal Parsec-Scale Jet of Markarian 501. *Astrophys. J. Lett.* **2002**, *579*, L67–L70. [[CrossRef](#)]
28. Homan, D.C.; Ojha, R.; Wardle, J.F.C.; Roberts, D.H.; Aller, M.F.; Aller, H.D.; Hughes, P.A. Parsec-Scale Blazar Monitoring: Proper Motions. *Astrophys. J.* **2001**, *549*, 840–861. [[CrossRef](#)]
29. Lister, M.L.; Homan, D.C.; Hovatta, T.; Kellermann, K.I.; Kiehlmann, S.; Kovalev, Y.Y.; Max-Moerbeck, W.; Pushkarev, A.B.; Readhead, A.C.S.; Ros, E.; et al. MOJAVE. XVII. Jet Kinematics and Parent Population Properties of Relativistically Beamed Radio-loud Blazars. *Astrophys. J.* **2019**, *874*, 43. [[CrossRef](#)]
30. Lister, M.L.; Homan, D.C.; Kellermann, K.I.; Kovalev, Y.Y.; Pushkarev, A.B.; Ros, E.; Savolainen, T. Monitoring Of Jets in Active Galactic Nuclei with VLBA Experiments. XVIII. Kinematics and Inner Jet Evolution of Bright Radio-loud Active Galaxies. *Astrophys. J.* **2021**, *923*, 30. [[CrossRef](#)]
31. Marscher, A.P. The compact jets of TeV blazars. *Astropart. Phys.* **1999**, *11*, 19–25. [[CrossRef](#)]
32. Britzen, S.; Witzel, A.; Gong, B.P.; Zhang, J.W.; Krishna, G.; Goyal, A.; Aller, M.F.; Aller, H.D.; Zensus, J.A. Understanding BL Lacertae objects. *Astron. Astrophys.* **2010**, *515*, A105. [[CrossRef](#)]
33. Wang, Z.; Wiita, P.J.; Hooda, J.S. Radio Jet Interactions with Massive Clouds. *Astrophys. J.* **2000**, *534*, 201–212. [[CrossRef](#)]
34. Hovatta, T.; Aller, M.F.; Aller, H.D.; Clausen-Brown, E.; Homan, D.C.; Kovalev, Y.Y.; Lister, M.L.; Pushkarev, A.B.; Savolainen, T. MOJAVE: Monitoring of Jets in Active Galactic Nuclei with VLBA Experiments. XI. Spectral Distributions. *Astron. J.* **2014**, *147*, 143. [[CrossRef](#)]
35. Gabuzda, D.C. Inherent and Local Magnetic Field Structures in Jets from Active Galactic Nuclei. *Galaxies* **2021**, *9*, 58. [[CrossRef](#)]
36. Laing, R.A.; Bridle, A.H. Relativistic models and the jet velocity field in the radio galaxy 3C 31. *Mon. Not. RAS* **2002**, *336*, 328–352. [[CrossRef](#)]
37. Sahayanathan, S. Boundary shear acceleration in the jet of MKN501. *Mon. Not. RAS* **2009**, *398*, L49–L53. [[CrossRef](#)]
38. Rieger, F.M.; Duffy, P. Particle Acceleration in Shearing Flows: Efficiencies and Limits. *Astrophys. J. Lett.* **2019**, *886*, L26. [[CrossRef](#)]
39. Pushkarev, A.B.; Aller, M.F.; Aller, H.D.; Homan, D.C.; Kovalev, Y.Y.; Lister, M.L.; Pashchenko, I.N.; Savolainen, T.; Zobnina, D. MOJAVE. XXI. Persistent Linear Polarization Structure in Parsec-scale AGN Jets. *arXiv* **2022**, arXiv:2209.04842.
40. Lisakov, M.M.; Kravchenko, E.V.; Pushkarev, A.B.; Kovalev, Y.Y.; Savolainen, T.K.; Lister, M.L. An Oversized Magnetic Sheath Wrapping around the Parsec-scale Jet in 3C 273. *Astrophys. J.* **2021**, *910*, 35. [[CrossRef](#)]
41. Gergely, L.Á.; Biermann, P.L. The Spin-Flip Phenomenon in Supermassive Black hole binary mergers. *Astrophys. J.* **2009**, *697*, 1621–1633. [[CrossRef](#)]
42. Kadowaki, L.H.S.; de Gouveia Dal Pino, E.M.; Medina-Torrejón, T.E.; Mizuno, Y.; Kushwaha, P. Fast Magnetic Reconnection Structures in Poynting Flux-dominated Jets. *Astrophys. J.* **2021**, *912*, 109. [[CrossRef](#)]
43. Medina-Torrejón, T.E.; de Gouveia Dal Pino, E.M.; Kadowaki, L.H.S.; Kowal, G.; Singh, C.B.; Mizuno, Y. Particle Acceleration by Relativistic Magnetic Reconnection Driven by Kink Instability Turbulence in Poynting Flux-Dominated Jets. *Astrophys. J.* **2021**, *908*, 193. [[CrossRef](#)]
44. Liska, M.; Hesp, C.; Tchekhovskoy, A.; Ingram, A.; van der Klis, M.; Markoff, S. Formation of precessing jets by tilted black hole discs in 3D general relativistic MHD simulations. *Mon. Not. RAS* **2018**, *474*, L81–L85. [[CrossRef](#)]
45. Gold, R.; Paschalidis, V.; Etienne, Z.B.; Shapiro, S.L.; Pfeiffer, H.P. Accretion disks around binary black holes of unequal mass: General relativistic magnetohydrodynamic simulations near decoupling. *Phys. Rev. D* **2014**, *89*, 064060. [[CrossRef](#)]
46. Lister, M.L.; Aller, M.F.; Aller, H.D.; Hodge, M.A.; Homan, D.C.; Kovalev, Y.Y.; Pushkarev, A.B.; Savolainen, T. MOJAVE. XV. VLBA 15 GHz Total Intensity and Polarization Maps of 437 Parsec-scale AGN Jets from 1996 to 2017. *Astrophys. J. Suppl.* **2018**, *234*, 12. [[CrossRef](#)]

**Disclaimer/Publisher’s Note:** The statements, opinions and data contained in all publications are solely those of the individual author(s) and contributor(s) and not of MDPI and/or the editor(s). MDPI and/or the editor(s) disclaim responsibility for any injury to people or property resulting from any ideas, methods, instructions or products referred to in the content.